



Published in final edited form as:

*Clin Cancer Res.* 2011 April 1; 17(7): 1713–1721. doi:10.1158/1078-0432.CCR-10-2081.

## Functional roles of Src and Fgr in ovarian carcinoma

Hye-Sun Kim<sup>1,2,\*</sup>, Hee Dong Han<sup>1,12,\*</sup>, Guillermo N. Armaiz-Pena<sup>1,\*</sup>, Rebecca L. Stone<sup>1</sup>, Eun Ji Nam<sup>1,3</sup>, Jeong-Won Lee<sup>1,4</sup>, Mian M. K. Shahzad<sup>1,5</sup>, Alpa M. Nick<sup>1</sup>, Sun Joo Lee<sup>1,6</sup>, Ju-Won Roh<sup>1,7</sup>, Masato Nishimura<sup>1</sup>, Lingegowda S. Mangala<sup>1,8</sup>, Justin Bottsford-Miller<sup>1</sup>, Gary E. Gallick<sup>9</sup>, Gabriel Lopez-Berestein<sup>10,11,12</sup>, and Anil K. Sood<sup>1,11,12</sup>

<sup>1</sup> Department of Gynecologic Oncology, U.T. M.D. Anderson Cancer Center, 1155 Herman Pressler, Unit 1362, Houston, TX 77030

<sup>2</sup> Department of Pathology, Cheil General Hospital and Women's Healthcare Center, Kwandong University College of Medicine, Seoul, Korea 100-380

<sup>3</sup> Women's Cancer Clinic, Department of Obstetrics and Gynecology, Yonsei University College of Medicine, Seoul, Korea 120-752

<sup>4</sup> Department of Obstetrics and Gynecology, Samsung Medical Center, Sungkyunkwan University School of Medicine, Seoul, Korea 135-710

<sup>5</sup> Department of Obstetrics and Gynecology, Division of Gynecologic Oncology and UW Carbone Cancer Center, University of Wisconsin, Madison, WI 53792

<sup>6</sup> Department of Obstetrics and Gynecology, Konkuk University Hospital, Konkuk University School of Medicine, Seoul, Korea

<sup>7</sup> Department of Obstetrics & Gynecology, Dongguk University Ilsan Hospital, Goyang, South Korea

<sup>8</sup> University of Space Research Association, NASA Johnson Space Center, Department of Radiation Biophysics, Houston, TX 77058

<sup>9</sup> Genitourinary Medical Oncology, U.T. M.D. Anderson Cancer Center, 1515 Holcombe Boulevard, Unit 0018-4, Houston, TX 77030

<sup>10</sup> Department of Experimental Therapeutics, U.T. M.D. Anderson Cancer Center, 1155 Herman Pressler, Unit 1362, Houston, TX 77030

<sup>11</sup> Department of Cancer Biology, U.T. M.D. Anderson Cancer Center, 1515 Holcombe Boulevard, Unit 173, Houston, TX 77030

<sup>12</sup> Center for RNA Interference and Non-coding RNA, The University of Texas M.D. Anderson Cancer Center

### Abstract

**Purpose**—Src is an attractive target because it is overexpressed in a number of malignancies, including ovarian cancer. However, the effect of Src silencing on other Src family kinases (SFKs) is not known. We hypothesized that other SFK members could compensate for the lack of Src activity.

---

Correspondence and Reprint Requests: Anil K. Sood, M.D., Professor, Departments of Gynecologic Oncology and Cancer Biology, The University of Texas, M.D. Anderson Cancer Center, 1155 Herman Pressler, Unit 1352, Houston, TX 77030 Phone: 713-745-5266; Fax: 713-792-7586; asood@mdanderson.org.

\*These authors contributed equally to this manuscript

**Experimental Design**—Cell viability following either Src or Fgr silencing was examined in ovarian cancer cell lines by MTT assay. Expression of SFKs after Src silencing in ovarian cancer cells was examined by real-time RT-PCR. Therapeutic effect of *in vivo* Src and/or Fgr silencing was examined using siRNA incorporated into chitosan nanoparticles (siRNA/CH-NP). Microvessel density (MVD), cell proliferation, and apoptosis markers were determined by immunohistochemical staining in ovarian tumor tissues.

**Results**—Src silencing enhanced cytotoxicity of docetaxel in both SKOV3ip1 and HeyA8 cells. In addition, Src silencing using siRNA/CH-NP in combination with docetaxel resulted in significant inhibition of tumor growth compared to control siRNA/CH-NP (81.8% reduction in SKOV3ip1,  $P = 0.017$ ; 84.3% reduction in HeyA8,  $P < 0.005$ ). These effects were mediated by decreased tumor cell proliferation and angiogenesis, and increased tumor cell apoptosis. Next, we assessed the effects of Src silencing on other SFK members in ovarian cancer cell lines. Src silencing resulted in significantly increased Fgr levels. Dual Src and Fgr silencing *in vitro* resulted in increased apoptosis that was mediated by increased caspase and AKT activity. In addition, dual silencing of Src and Fgr *in vivo* using siRNA/CH-NP resulted in the greatest reduction in tumor growth compared to silencing of either Src or Fgr alone in the HeyA8 model (68.8%,  $P < 0.05$ ).

**Conclusions**—This study demonstrates that, in addition to Src, Fgr plays a biologically significant role in ovarian cancer growth and might represent an important target.

### Keywords

Src; Fgr; ovarian cancer; chitosan nanoparticles; siRNA

### Introduction

Ovarian cancer is the fifth leading cause of cancer death in women in the United States with an estimated 21,550 new cases diagnosed in 2009, and 14,600 deaths (1). The high mortality for ovarian cancer has changed little despite improvements in surgical and chemotherapeutic approaches. The main reasons for high mortality rates associated with ovarian cancer are advanced disease at the time of diagnosis and high recurrence rates after initial treatment (2). Therefore, new therapeutic approaches are needed to improve the outcome of women with ovarian cancer.

Src family kinases (SFKs) comprise a subclass of membrane-associated non-receptor tyrosine kinases that are involved in a variety of cellular processes important for cancer growth and progression, such as cell division, motility, adhesion, angiogenesis, and survival (3,4). Several of the SFKs have been shown to be upregulated in cancer and promote progression and metastasis. Among SFKs, Src has arguably been the best characterized and most often implicated in cancer. Furthermore, Src is a particularly attractive target because it is overexpressed in a number of malignancies, including ovarian cancer (5). Even though Src is the most widely studied SFK, there remains a void in understanding how other SFKs might relate to Src-mediated functions and potentially contribute to redundant pathways.

Emerging data suggest that SFKs play key roles in tumor growth and progression. Among these, Fgr localizes to plasma membrane ruffles, and functions as a negative regulator of cell migration and adhesion triggered by the beta-2 integrin signal transduction pathway. Moreover, Fgr is overexpressed in hematopoietic cells and associated with adhesion and migration of granulocytes (6–10). Recently, Fgr overexpression was found to be associated with aggressive tumor features, and shorter overall survival among patients with leukemia (11), lymphoma (12), or glioblastoma multiforme (13). However, the role of Fgr in cancer treatment is not known.

Here, we sought to determine whether other SFK members could compensate for the lack of Src activity. Our findings demonstrate that Src and Fgr play key roles in ovarian cancer growth and progression. Moreover, dual silencing of Src and Fgr results in increased apoptosis and effective anti-tumor activity.

## Materials and Methods

### Cell lines

The ovarian cancer cell lines, HeyA8 and SKOV3ip1, were maintained and propagated in RPMI 1640 supplemented with 15% fetal bovine serum and 0.1% gentamicin sulfate (Gemini Bioproducts, Calabasas, CA). The taxane-resistant HeyA8-MDR cells were a generous gift from Dr. Isaiah J. Fidler, Department of Cancer Biology, University of Texas M. D. Anderson Cancer Center, Houston, TX. They were maintained in RPMI 1640 supplemented with 15% fetal bovine serum and 300 ng/ml paclitaxel. All *in vitro* and *in vivo* experiments were conducted when cells were 70% to 80% confluent.

### SiRNA

Target sequences for Src (5'-GGGCGAACCACCUGAACAA-3'), Fgr (5'-GACAUGGGCGGCUACUACA-3'), and Control (5'-UUCUCCGAACGUGUCACGU-3') were purchased from Sigma Genosys (The Woodlands, TX).

### Western blot

Preparation of cell and tumor tissue lysates has been previously described (14). Protein concentrations were determined using a BCA Protein Assay Reagent Kit (Pierce Biotech., Rockford, IL) and aliquots of 20  $\mu$ g protein were subjected to gel electrophoresis on 7.5% or 10% SDS-PAGE gels. Transfer to membranes and immunoblotting were performed as described previously (14).

### Cell viability assay

Cells were plated on 96-well plates in triplicate and incubated for 24 hr at 37°C and 5% CO<sub>2</sub>. After incubation, cells were washed, serum and antibiotic-free medium added and treated with control, Src, or Fgr siRNA. After 6 hours, cells were washed and incubated in serum-containing medium overnight. Afterwards, cells were washed and either regular or docetaxel containing medium were added. After 72 hours, cell viability was determined by the 3-(4,5-dimethylthiazol-2-yl)-2,5-diphenyltetrazolium bromide (MTT) assay (15).

### Real-time RT-PCR

Relative expression of SFKs (Src, Fgr, Fyn, Hck, Lyn, and Yes) mRNA after Src silencing was determined by real-time quantitative PCR analysis of total RNA isolated from HeyA8 using the RNeasy Mini Kit (Qiagen, Valencia, CA) following the manufacturer's protocol. Fold change for relative expression was calculated using the  $2^{-\Delta\Delta CT}$  method, as previously described (16).

### Cell apoptosis

Relative percentage of apoptotic cells was assessed by propidium iodide (PI) staining, as previously described (15). Briefly, SKOV3ip1 cells (10<sup>6</sup> cells/ml) were pelleted and washed twice in PBS and resuspended in PBS containing PI (5  $\mu$ l per 10<sup>5</sup> cells). Samples were incubated in the dark for 15 min at room temperature before being analyzed by flow cytometry.

## Cell migration and invasion assays

Cell migration and invasion assays have been previously described (17). Briefly, cells were treated with either control, Fgr, Src, or combination of Fgr and Src siRNA for 24 hours. Then, cells were re-suspended in serum-free medium ( $1 \times 10^6$  cells/ml), and 1 ml added to gelatin-coated inserts. The inserts were then transferred to wells filled with serum-containing media. Cells were allowed to migrate for 6 hours at 37°C. Cells that had migrated into the bottom wells were collected, fixed, stained, and counted by light microscopy. Cells were counted in 10 random fields ( $\times 200$  final magnification) and the average number of cells determined.

For invasion assays, cells were treated with control, Fgr, Src, or combination of Fgr and Src siRNA for 36 hours. Then, cells were re-suspended in serum-free medium ( $5 \times 10^5$  cells/ml), and 1 ml added to inserts coated with a defined matrix consisting of human laminin, type IV collagen, and gelatin (17). Inserts were then transferred to wells filled with serum-containing media. Cells were then allowed to invade for 24 hours at 37°C. Cells that had migrated into the bottom wells were collected, fixed, stained, and counted by light microscopy. Cells were counted in 10 random fields ( $\times 200$  final magnification) and the average number of cells determined.

## Preparation of siRNA incorporated chitosan nanoparticles (siRNA/CH-NP)

siRNA/CH-NP was prepared based on ionic gelation of anionic tripolyphosphate (TPP) and siRNA, as previously described (18,19). Briefly, predetermined TPP (0.25% w/v) and siRNA (1  $\mu\text{g}/\mu\text{l}$ ) were added into a chitosan solution. After constant stirring at room temperature, siRNA/CH-NP was formed. The siRNA/CH-NP was collected by centrifugation following an incubation of 40 min at 4°C. The pellet was washed 3 times to remove unbound chemicals or siRNA. The siRNA/CH-NP was stored at 4°C until needed.

## *In vivo* tumor model and tissue processing

Female athymic nude mice (NCr-nu) were purchased from the National Cancer Institute-Frederick Cancer Research and Development Center (Frederick, MD) and housed in specific pathogen-free conditions. They were cared for in accordance with guidelines set forth by the American Association for Accreditation of Laboratory Animal Care and the USPHS Policy on Human Care and Use of Laboratory Animals, and all studies were approved and supervised by the M. D. Anderson Cancer Center Institutional Animal Care and Use Committee. For *in vivo* experiments, ovarian cancer cells were harvested with trypsin-EDTA (Life Technologies, Carlsbad, CA) and centrifuged at 1,200 rpm for 5 min at 4°C, then washed twice with PBS, and reconstituted in the appropriate volume of HBSS (Life Technologies) for a final concentration of  $2.5 \times 10^5$  cells/mouse for HeyA8 or  $1 \times 10^6$  cells/mouse for SKOV3ip1 and HeyA8-MDR. Tumor was established by i.p. injections.

To assess tumor growth, treatment began 1 week after injection of tumor cells. Mice were randomly divided into 4 groups ( $n = 10$  mice per group) for the Src silencing experiment: (a) control siRNA/CH-NP + PBS, (b) control siRNA/CH-NP + docetaxel, (c) Src siRNA/CH-NP + PBS, and (d) Src siRNA/CH-NP + docetaxel. For dual silencing of Src and Fgr, mice were also randomly divided into 4 groups ( $n = 10$  mice per group): (a) control siRNA/CH-NP, (b) Src siRNA/CH-NP, (c) Fgr siRNA/CH-NP, and (d) Src and Fgr siRNA/CH-NP. Each siRNA/CH-NP was injected intravenously twice a week at a dose of 150  $\mu\text{g}/\text{kg}$  body weight and docetaxel was injected into the peritoneal cavity once a week at a dose of 2 mg/kg (HeyA8 and HeyA8-MDR) or 1.4 mg/kg (SKOV3ip1). Mice were sacrificed after they became moribund (typically 4 to 5 weeks depending on tumor cell type). Tumor weight, number of tumor nodules, and distribution of tumors were recorded. Tumor tissue was snap-frozen for protein analysis or immersed in optimum cutting temperature (OCT) medium for

frozen slide preparations. Tumor specimens were also fixed in formalin for paraffin slide preparation.

### Immunohistochemical staining

Immunohistochemical analysis for CD31 and Ki67 was performed as previously described (20). To quantify microvessel density (MVD), the number of blood vessels staining positive for CD31 was recorded in 5 random fields at  $\times 200$  magnification for each sample. For Ki67, the number of positive cells and the total number of cells were counted in 5 random fields at  $\times 200$  magnification for each sample. Terminal deoxynucleotidyl transferase-mediated deoxyuridine triphosphate nick-end labeling (TUNEL) stain was performed on frozen tissue using Promega Kit (Promega, Madison, WI) and cells were counterstained in 5 random fields at  $\times 200$  magnification (20).

### Statistical analyses

Differences in continuous variables were analyzed using the student's t-test or ANOVA as appropriate. For values that were not normally distributed, the Mann-Whitney rank sum test was used. A  $P$  value of  $<0.05$  was considered statistically significant. The statistical package for the Social Sciences (SPSS, Inc.) was used for all statistical analyses.

## Results

### *In vitro* Src silencing

Prior to testing the *in vivo* biological effect of Src gene silencing, we first tested the *in vitro* effects on SKOV3ip1 and HeyA8 cells. Both cell lines were harvested at time points ranging from 24–96 hours after transfection with Src siRNA and the expression of total Src was determined by Western blot (Fig. 1A). The protein expression of Src reached maximum down-regulation between 48 and 72 hours in the SKOV3ip1 and HeyA8 cells (Fig. 1A). As expected, Src silencing resulted in decreased phosphorylation of downstream proteins such as FAK (Supplementary Fig. S1). We have previously reported that a Src-targeted small molecule inhibitor can sensitize ovarian cancer cells to taxanes (5). Since small molecule inhibitors can have non-specific effects, we examined the effects of Src gene silencing on cell viability. Src silencing enhanced the cytotoxicity of docetaxel in both SKOV3ip1 and HeyA8 cells across a range of concentrations. In both cell lines, Src silencing resulted in lower cell viability compared to the no treatment and control siRNA groups ( $P < 0.05$ ; Fig. 1B).

### Therapeutic efficacy of Src silencing

Based on prior *in vitro* data, we next assessed *in vivo* therapeutic efficacy of Src silencing. For systemic delivery of siRNA, we have recently developed a highly efficient method using chitosan nanoparticles (19). Seven days following i.p. injection of tumor cells, mice were randomly allocated to one of four treatment groups. Mice were sacrificed when animals in any group became moribund. As expected, tumor growth was significantly reduced in the control siRNA/CH-NP + docetaxel group (Fig. 2A). Src siRNA/CH-NP + PBS also resulted in significant growth inhibition compared to control siRNA/CH-NP + PBS (52.8% and 51.8% reduction in SKOV3ip1; 57.9% and 38.5% reduction in HeyA8; Fig. 2A and B). Combination of Src siRNA/CH-NP + docetaxel resulted in the greatest tumor reduction compared to control siRNA/CH-NP + PBS (81.8% reduction in SKOV3ip1,  $P = 0.017$ ; 84.3% reduction in HeyA8,  $P < 0.005$ ; Fig. 2A and B).

Given the suspected role for Src in resistance to chemotherapy, we also examined the effects of Src gene silencing in the taxane-resistant HeyA8-MDR model (Fig. 2C). Src siRNA/CH-NP + PBS reduced tumor growth by 71.2% compared to control siRNA/CH-NP + PBS.

Additionally, combination treatment of Src siRNA/CH-NP with docetaxel resulted in 92.3% reduction of tumor growth compared to control siRNA/CH-NP + PBS ( $P = 0.02$ ; Fig. 2C).

To determine potential mechanisms responsible for the therapeutic effects of Src silencing and docetaxel, we examined tumor cell proliferation (Ki67), tumor associated microvessel density (MVD, CD31 staining), and tumor cell apoptosis (TUNEL) (Fig. 2D and Supplementary Fig. S2). Tumor cell proliferation was significantly reduced in the Src siRNA/CH-NP + docetaxel group compared to the control siRNA/CH-NP + PBS group (25% reduction,  $P < 0.001$ ; Fig. 2D). Similar effects were observed in the HeyA8 and HeyA8-MDR models (Supplementary Fig. S2). Additionally, MVD was significantly reduced in both SKOV3ip1 and HeyA8 models (Fig. 2D and Supplementary Fig. S2A); however, the greatest reduction was noted in the combination group (75% and 60% reduction in the SKOV3ip1 and HeyA8 models, respectively,  $P < 0.001$ ). In the HeyA8-MDR model, there was no significant reduction with control siRNA/CH-NP + PBS or control siRNA/CH-NP + docetaxel ( $P = 0.17$ ), however, combination treatment resulted in significantly decreased MVD compared to control siRNA/CH-NP + PBS (42.9%,  $P < 0.001$ ; Supplementary Fig. S2B). Notably, combined treatment of Src siRNA/CH-NP + docetaxel resulted in a significant increase in tumor cell apoptosis compared to control siRNA/CH-NP + PBS ( $P < 0.001$  for both SKOV3ip1 and HeyA8,  $P = 0.02$  for HeyA8-MDR; Fig. 2D and Supplementary Fig. S2).

### Src silencing increases Fgr levels

We next considered whether other SFKs levels are affected by Src silencing. Therefore, we analyzed changes in mRNA expression levels of other SFKs members (Src, Fgr, Fyn, Hck, Lyn and Yes) in response to Src silencing (Fig. 3A). Following Src silencing, Fgr mRNA levels was increased by 2-fold compared to controls at 96 hours. In addition, we observed similar effects of Src silencing on Fgr protein levels (Fig. 3B). Since Fgr mRNA levels were significantly increased after Src silencing, we considered whether Fgr might play a complementary role to Src. On the basis of these results, we next examined the *in vitro* and *in vivo* effects of simultaneously silencing Src and Fgr.

For testing the *in vitro* effects of Fgr silencing, a siRNA sequence was designed that reduced Fgr expression by >90% after 72 hours compared to control siRNA (Fig. 3C). Subsequently, we sought to determine whether Fgr silencing could sensitize ovarian cancer cells to chemotherapy. Based on cell viability assays, Fgr silencing enhanced the cytotoxic effect combined with docetaxel (Fig. 3D). Subsequently, we assessed whether dual Src and Fgr silencing could promote tumor cell apoptosis. While Src or Fgr silencing individually did not result in increased tumor cell apoptosis, dual silencing resulted in significantly increased tumor cell apoptosis by more than 2-fold compared to all other groups ( $P < 0.01$ ; Fig. 4A and Supplementary Fig. S3). To identify potential pathways that could be responsible for the increased rate of apoptosis after dual Src and Fgr silencing, we analyzed the activity of several known pro-apoptotic proteins by Western blot (Fig. 4B). Caspase 3, 8 and 9 levels were increased after dual Src and Fgr silencing. Moreover, AKT activity was also significantly increased after dual Src and Fgr silencing (Fig. 4B), suggesting that the increase in tumor cell apoptotic rate after dual silencing might be mediated by the activation of AKT and caspases. In addition, we tested effects of small molecule inhibitors such as PP2 and dasatinib on Src activity and Fgr levels. Treatment of ovarian cancer cells with these inhibitors also resulted in increased Fgr levels (Supplementary Fig. S4). These data indicate that dual Src and Fgr silencing results in increased apoptosis through caspase activation. We also examined the effects of dual Src and Fgr silencing on cancer cell migration and invasion. Dual silencing resulted in significantly decreased cell migration and invasion, however, these effects were similar to silencing each gene individually (Supplementary Fig. S5).

On the basis of the *in vitro* findings noted above, we next examined the *in vivo* effects of dual Src and Fgr silencing using Src siRNA/CH-NP and Fgr siRNA/CH-NP. Mice were injected i.p. with HeyA8 ovarian cancer cells and randomly divided into the following treatment groups 7 days after injection (n=10 mice per group): control siRNA/CH-NP, Src siRNA/CH-NP, Fgr siRNA/CH-NP or Src/Fgr siRNA/CH-NP. Both Src and Fgr siRNA/CH-NP inhibited tumor growth compared to the control siRNA/CH-NP group (41.9% and 40.5%, respectively; Fig. 5A). Moreover, dual Src and Fgr silencing resulted in the greatest inhibition in tumor growth compared to control siRNA/CH-NP (68.8% reduction,  $P < 0.005$ ; Fig. 5A).

To examine potential mechanisms responsible for the decrease in tumor growth after dual Src and Fgr silencing, we examined tumor cell proliferation, microvessel density and apoptosis (Fig. 5B). Tumor cell proliferation was significantly reduced in the dual Src and Fgr silencing group compared to the control group ( $P < 0.001$ ). Additionally, tumor associated microvessel density was significantly decreased ( $P < 0.001$ ), suggesting that dual Src and Fgr silencing might decrease angiogenesis. Dual Src and Fgr silencing also resulted in a significant increase in tumor cell apoptosis compared to the control group ( $P < 0.001$ ; Fig. 5B).

## Discussion

The key findings from this study are that Fgr levels increase significantly following Src silencing and dual Src and Fgr silencing is effective in reducing ovarian cancer growth *in vivo*. These effects were achieved, in part, through decreased tumor cell proliferation and angiogenesis and increased tumor cell apoptosis that was mediated by increased caspase and AKT activity. The *in vivo* effects of Src silencing were more pronounced compared to *in vitro* effects, which is not surprising given the direct (on tumor cells) and indirect (e.g., effects of reduced angiogenesis) effects. These findings suggest that, in addition to targeting Src, Fgr might represent an important target in ovarian cancer.

Src family kinases are a group of membrane-associated non-receptor tyrosine kinases that are involved in a variety of cellular functions including cell proliferation, invasion, migration, and apoptosis (4). Src has been found to be overexpressed in a majority of late stage human ovarian cancers (21,22) and to promote survival and resistance against chemotherapy (23). In the current study, we demonstrate that Src silencing inhibited tumor growth compared to controls. The addition of docetaxel further enhanced inhibition of tumor growth compared to controls, even in chemo-resistant models. However, despite the known role of Src in tumor growth and angiogenesis (5,23–25), Src inhibitors have only had modest success (5,26), suggesting the presence of compensatory factors. Among these, we found that Fgr levels were significantly increased after Src silencing. Fgr is a member of SFKs, which plays a role in cell migration and adhesion triggered by the beta-2 integrin signal transduction pathway in monocytes. Fgr has been known to be overexpressed in hematopoietic cells, and is associated with granulocyte adhesion and migration (6–10). However, Fgr's role in cancer cells has not been sufficiently studied. Some studies suggest that Fgr might play a complementary role to Src and represent a potential therapeutic target (11,27). Our findings extend previous knowledge by demonstrating that Fgr levels are significant increases following Src silencing in ovarian cancer cells. Moreover, this increase in Fgr might compensate for some of Src's functions in cancer cells since gene silencing of both kinases compromised cell survival to a greater extent. It is possible that such increases in Fgr might limit the efficacy of Src targeted drugs.

While a number of important targets in tumor and endothelial cells have been identified, many of these are difficult to target with small molecule inhibitors or monoclonal

antibodies. This limitation prompted us to consider RNA interference as a therapeutic modality, which holds great potential for cancer therapy. We have recently developed chitosan nanoparticles that allow efficient systemic delivery of siRNA into orthotopic tumors (18,19). Chitosan is highly desirable for biological applications due to properties such as low immunogenicity and low toxicity (28–30).

Here, we demonstrate that dual Src and Fgr silencing is an effective approach for treatment of ovarian carcinoma in animal models. Dual Src and Fgr silencing further decreased tumor microvessel density (angiogenesis), cell survival (increased apoptosis), and tumor growth. In addition, these effects might be mediated by increased caspase and AKT activity. Such combinations warrant further development in ovarian and other cancers.

## Supplementary Material

Refer to Web version on PubMed Central for supplementary material.

## Acknowledgments

**Grant support:** Portions of this work were supported by NIH grants (CA 110793, 109298, CA 128797, and RC2 GM 092599, U54 CA151668), DOD (OC-073399, W81 XWH-10-1-0158, BC 085265), the Ovarian Cancer Research Fund, Inc. (Program Project Development Grant), U.T.M.D. Anderson Cancer Center SPORE (P50CA083639), the Zarrow Foundation, the Marcus Foundation, and the Betty Anne Asche Murray Distinguished Professorship. AMN, JBM, and RS are supported by NCI-DHHS-NIH T32 Training Grant (T32 CA101642). MMS was supported by the Baylor WRHR grant (HD050128) and the GCF Molly-Cade ovarian cancer research grant.

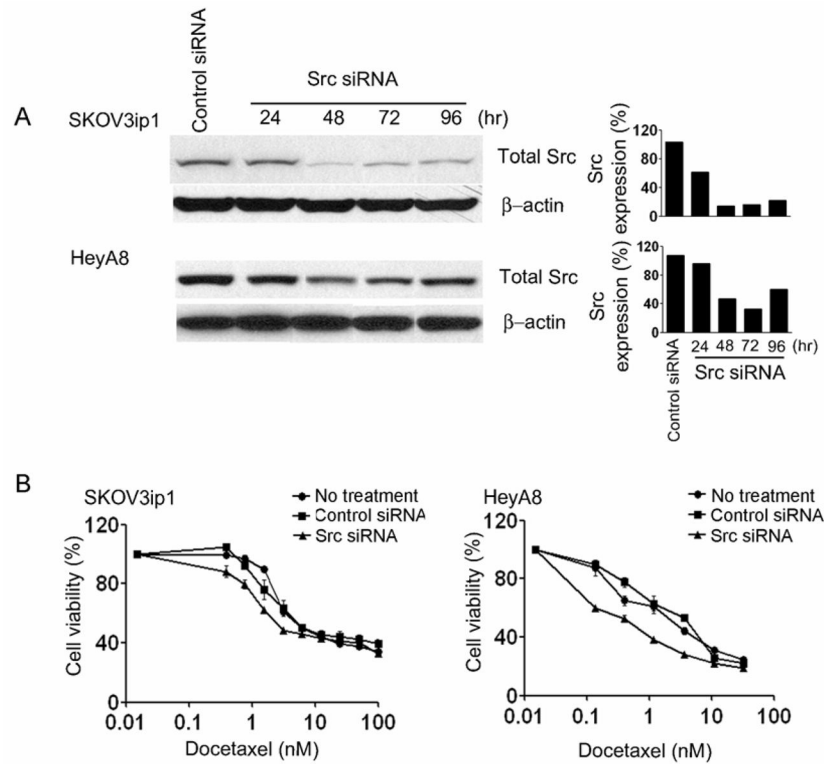
The authors thank Nicholas B. Jennings and Donna Reynolds for their technical expertise.

## References

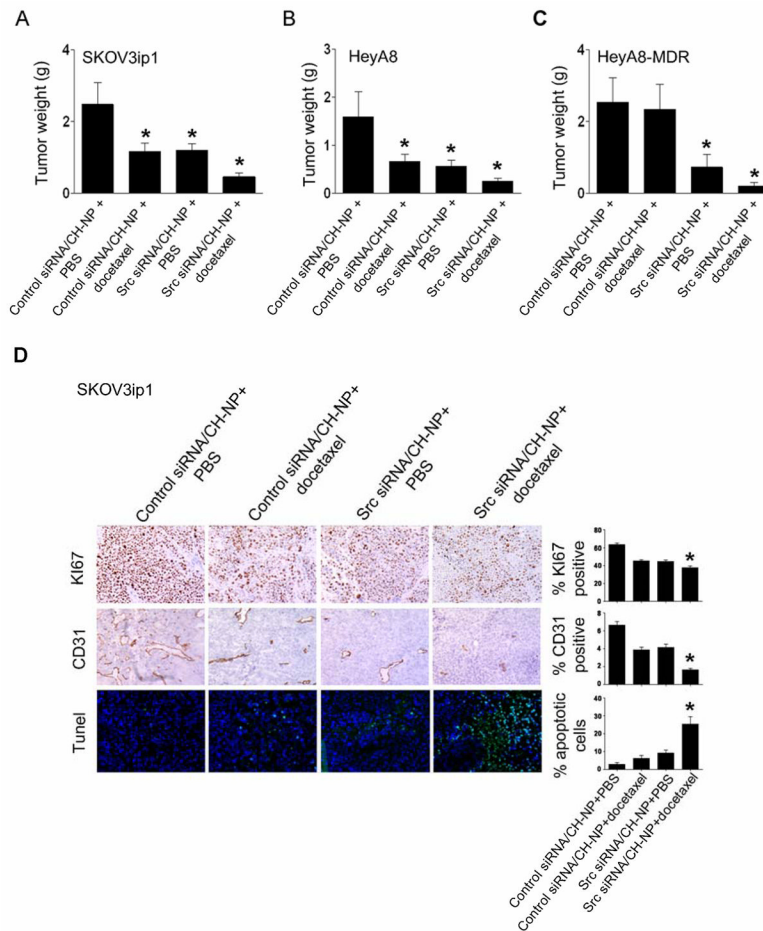
1. Society, AC. Cancer facts and figures—2009. Atlanta, GA: American Cancer Society; 2009.
2. Barnes MN, Grizzle WE, Grubbs CJ, Partridge EE. Paradigms for primary prevention of ovarian carcinoma. *CA Cancer J Clin.* 2002; 52(4):216–25. [PubMed: 12139233]
3. Parsons SJ, Parsons JT. Src family kinases, key regulators of signal transduction. *Oncogene.* 2004; 23(48):7906–9. [PubMed: 15489908]
4. Thomas SM, Brugge JS. Cellular functions regulated by Src family kinases. *Annu Rev Cell Dev Biol.* 1997; 13:513–609. [PubMed: 9442882]
5. Han LY, Landen CN, Trevino JG, et al. Antiangiogenic and antitumor effects of SRC inhibition in ovarian carcinoma. *Cancer Res.* 2006; 66(17):8633–9. [PubMed: 16951177]
6. Lowell CA, Fumagalli L, Berton G. Deficiency of Src family kinases p59/61hck and p58c-fgr results in defective adhesion-dependent neutrophil functions. *J Cell Biol.* 1996; 133(4):895–910. [PubMed: 8666673]
7. Mocsai A, Ligeti E, Lowell CA, Berton G. Adhesion-dependent degranulation of neutrophils requires the Src family kinases Fgr and Hck. *J Immunol.* 1999; 162(2):1120–6. [PubMed: 9916742]
8. Suen PW, Ilic D, Cavegion E, Berton G, Damsky CH, Lowell CA. Impaired integrin-mediated signal transduction, altered cytoskeletal structure and reduced motility in Hck/Fgr deficient macrophages. *J Cell Sci.* 1999; 112 (Pt 22):4067–78. [PubMed: 10547366]
9. Gresham HD, Dale BM, Potter JW, et al. Negative regulation of phagocytosis in murine macrophages by the Src kinase family member, Fgr. *J Exp Med.* 2000; 191(3):515–28. [PubMed: 10662797]
10. Baruzzi A, Cavegion E, Berton G. Regulation of phagocyte migration and recruitment by Src-family kinases. *Cell Mol Life Sci.* 2008; 65(14):2175–90. [PubMed: 18385944]
11. Hu Y, Liu Y, Pelletier S, et al. Requirement of Src kinases Lyn, Hck and Fgr for BCR-ABL1-induced B-lymphoblastic leukemia but not chronic myeloid leukemia. *Nat Genet.* 2004; 36(5): 453–61. [PubMed: 15098032]



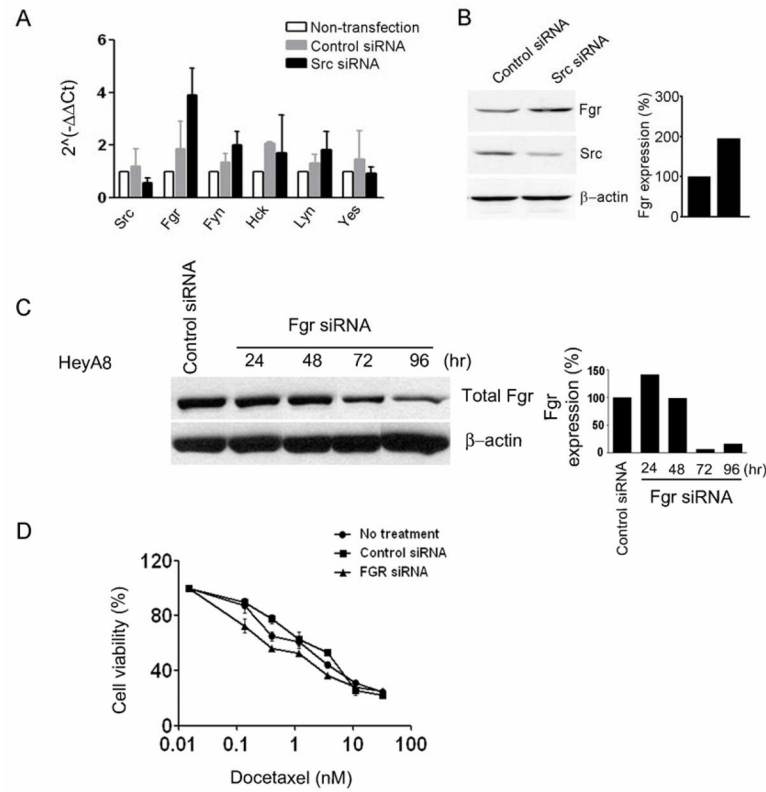
12. Sharp NA, Luscombe MJ, Clemens MJ. Regulation of c-fgr proto-oncogene expression in Burkitt's lymphoma cells: effect of interferon treatment and relationship to EBV status and c-myc mRNA levels. *Oncogene*. 1989; 4(8):1043–6. [PubMed: 2548145]
13. Hui AB, Lo KW, Yin XL, Poon WS, Ng HK. Detection of multiple gene amplifications in glioblastoma multiforme using array-based comparative genomic hybridization. *Lab Invest*. 2001; 81(5):717–23. [PubMed: 11351043]
14. Mangala LS, Zuzel V, Schmandt R, et al. Therapeutic Targeting of ATP7B in Ovarian Carcinoma. *Clin Cancer Res*. 2009; 15(11):3770–80. [PubMed: 19470734]
15. Lee JW, Han HD, Shahzad MM, et al. EphA2 immunoconjugate as molecularly targeted chemotherapy for ovarian carcinoma. *J Natl Cancer Inst*. 2009; 101(17):1193–205. [PubMed: 19641174]
16. Livak KJ, Schmittgen TD. Analysis of relative gene expression data using real-time quantitative PCR and the 2(-Delta Delta C(T)) Method. *Methods*. 2001; 25(4):402–8. [PubMed: 11846609]
17. Spannuth WA, Nick AM, Jennings NB, et al. Functional significance of VEGFR-2 on ovarian cancer cells. *Int J Cancer*. 2009; 124(5):1045–53. [PubMed: 19058181]
18. Han HD, Mangala LS, Lee JW, et al. Targeted gene silencing using RGD-labeled chitosan nanoparticles. *Clin Cancer Res*. 2010; 16(15):3910–22. [PubMed: 20538762]
19. Lu C, Han HD, Mangala LS, et al. Regulation of tumor angiogenesis by EZH2. *Cancer Cell*. 2010; 18(2):185–97. [PubMed: 20708159]
20. Shahzad MM, Lu C, Lee JW, et al. Dual targeting of EphA2 and FAK in ovarian carcinoma. *Cancer Biol Ther*. 2009; 8(11):1027–34. [PubMed: 19395869]
21. Wiener JR, Windham TC, Estrella VC, et al. Activated SRC protein tyrosine kinase is overexpressed in late-stage human ovarian cancers. *Gynecol Oncol*. 2003; 88(1):73–9. [PubMed: 12504632]
22. Budde RJ, Ke S, Levin VA. Activity of pp60c-src in 60 different cell lines derived from human tumors. *Cancer Biochem Biophys*. 1994; 14(3):171–5. [PubMed: 7537173]
23. Pengetnze Y, Steed M, Roby KF, Terranova PF, Taylor CC. Src tyrosine kinase promotes survival and resistance to chemotherapeutics in a mouse ovarian cancer cell line. *Biochem Biophys Res Commun*. 2003; 309(2):377–83. [PubMed: 12951060]
24. Chen T, Pengetnze Y, Taylor CC. Src inhibition enhances paclitaxel cytotoxicity in ovarian cancer cells by caspase-9-independent activation of caspase-3. *Mol Cancer Ther*. 2005; 4(2):217–24. [PubMed: 15713893]
25. Wiener JR, Nakano K, Kruzlock RP, Bucana CD, Bast RC Jr, Gallick GE. Decreased Src tyrosine kinase activity inhibits malignant human ovarian cancer tumor growth in a nude mouse model. *Clin Cancer Res*. 1999; 5(8):2164–70. [PubMed: 10473101]
26. Nam S, Kim D, Cheng JQ, et al. Action of the Src family kinase inhibitor, dasatinib (BMS-354825), on human prostate cancer cells. *Cancer Res*. 2005; 65(20):9185–9. [PubMed: 16230377]
27. Edwards J, Krishna NS, Witton CJ, Bartlett JM. Gene amplifications associated with the development of hormone-resistant prostate cancer. *Clin Cancer Res*. 2003; 9(14):5271–81. [PubMed: 14614009]
28. Han HD, Song CK, Park YS, et al. A chitosan hydrogel-based cancer drug delivery system exhibits synergistic antitumor effects by combining with a vaccinia viral vaccine. *Int J Pharm*. 2008; 350(1–2):27–34. [PubMed: 17897800]
29. Seo SH, Han HD, Noh KH, Kim TW, Son SW. Chitosan hydrogel containing GMCSF and a cancer drug exerts synergistic anti-tumor effects via the induction of CD8+ T cell-mediated anti-tumor immunity. *Clin Exp Metastasis*. 2009; 26(3):179–87. [PubMed: 19082918]
30. Han HD, Nam DE, Seo DH, Kim TW, Shin BC, Choi HS. Preparation and biodegradation of thermosensitive chitosan hydrogel as a function of pH and temperature. *Macromol Res*. 2004; 12:507–11.



**Fig. 1.** *In vitro* effect of Src silencing by Src siRNA. A, Western blot analysis of Src in SKOV3ip1 and HeyA8 cells following transfection with Src siRNA for 24, 48, 72, and 96 hours. Protein levels were quantified by densitometry and expression is shown as % expression of Src. B, Cell viability after Src siRNA transfection combined with docetaxel on SKOV3ip1 and HeyA8 cells. Error bar represent SEM.



**Fig. 2.** Therapeutic efficacy of Src siRNA/CH-NP. Mice injected with A, SKOV3ip1, B, HeyA8, or C, HeyA8-MDR cells were initiated in control siRNA/CH-NP, Src siRNA/CH-NP twice a week, docetaxel once a week, and combination of Src siRNA/CH-NP and docetaxel. Treatments were started 1 week after tumor cell injection and siRNA/CH-NP injected twice weekly at a dose of 150  $\mu\text{g}/\text{kg}$  body weight and docetaxel 35  $\mu\text{g}$  for SKOV3ip1 and 50  $\mu\text{g}$  for HeyA8 tumor model. All of the animals were sacrificed when animals in any group appeared moribund. Statistical analysis for tumor weights was done by Student's *t* test,  $P < 0.05$ . D, *In vivo* effects of Src silencing on tumor cell proliferation, angiogenesis, and apoptosis. Immunohistochemical stains for cell proliferation and angiogenesis, and TUNEL stain for apoptosis were performed on SKOV3ip1-bearing mice.

**Fig. 3.**

A, Effect of Src silencing on the SFKs in ovarian cancer cell line. Real-time RT-PCR was performed in HeyA8 cells to evaluate the expression level of mRNA of SFKs after Src silencing (96 hours). B, Western Blot analysis demonstrating the effect of Src silencing on Fgr protein levels. C, *In vitro* effects of Fgr silencing by Fgr siRNA was observed by Western blot in HeyA8 cells. D, Effect of Fgr silencing in combination with docetaxel on ovarian cancer cell viability. Error bar represent SEM.

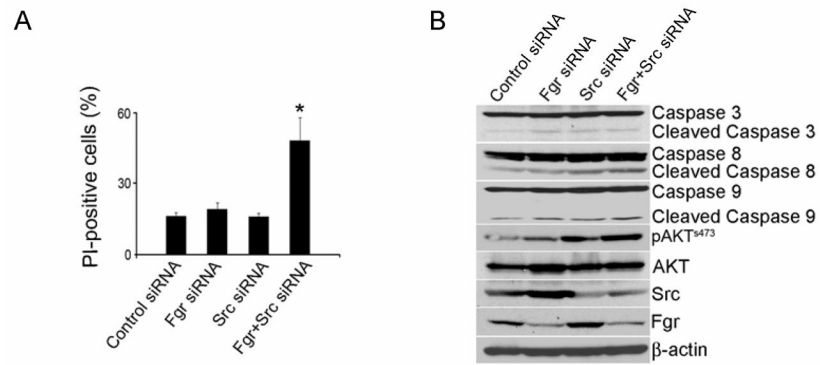


**Fig. 4.** Effect of Src and Fgr silencing on SKOV3ip1. A, Apoptosis was measured as the percentage of PI-positive cells. Error bar represent SEM,  $P < 0.05$ . B, After dual silencing of Src and Fgr, SKOV3ip1 lysate was analyzed by western blot for AKT and caspase 3, 8, and 9 activity.

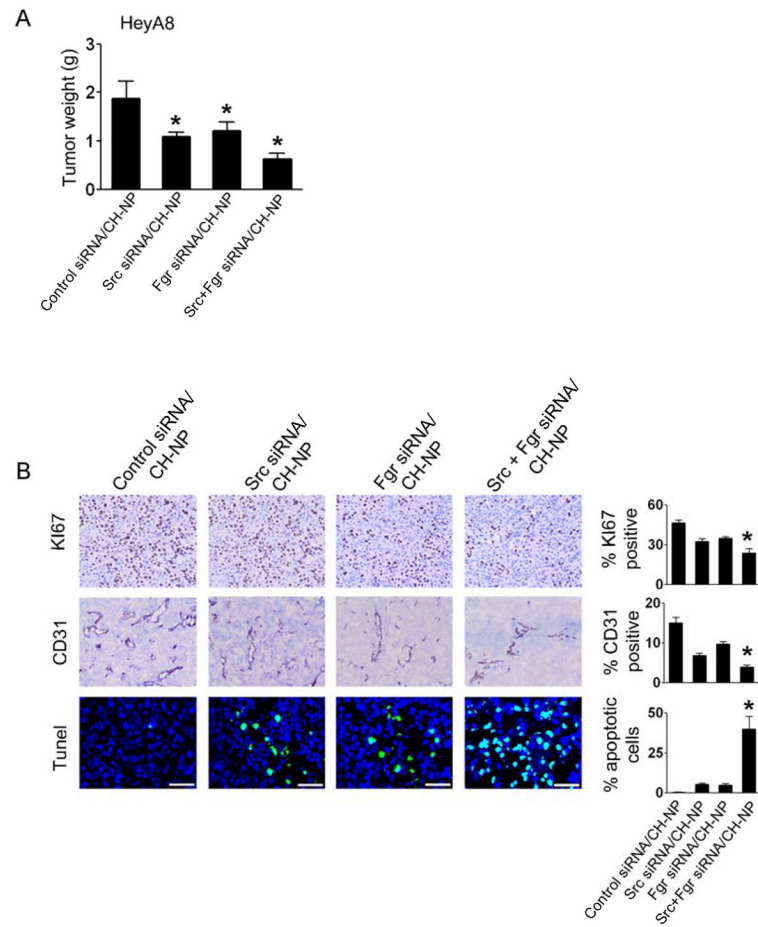


**Fig. 5.** *In vivo* effects of Src and Fgr silencing. A, Mean tumor weights with treatment of Src or Fgr siRNA/CH-NP alone or combination. Mice injected with HeyA8 cells were treated with control siRNA/CH-NP, Src siRNA/CH-NP, Fgr siRNA/CH-NP, or combined Src and Fgr siRNA/CH-NP twice a week. B, Immunohistochemical stains for cell proliferation and angiogenesis, and TUNEL stain for apoptosis were performed on HeyA8 tumors. Error bar represent SEM,  $P < 0.05$ .